EXPERIMENTS AND FINITE ELEMENT ANALYSIS OF THE STRUCTURAL BEHAVIOR OF REINFORCED HIGH STRENGTH CONCRETE STUB COLUMNS

Christina Claeson
Research Assistant, M.Sc.
Division of Concrete Structures
Chalmers University of Technology
S-412 96 Göteborg, Sweden

Kent Gylltoft
Ph.D., Professor
Division of Concrete Structures
Chalmers University of Technology
S-412 96 Göteborg, Sweden

ABSTRACT

An experimental study of the behavior of reinforced concrete columns and results of numerical and non-linear finite element analyses are presented. 26 stub columns were tested under centric and eccentric monotonic loading. Effects of key parameters such as concrete strength, stirrup spacing, reinforcement strength and eccentricity of the applied axial load were studied. Important gains in load bearing capacity were obtained with increased concrete strength. The results of the finite element analyses correlate well with the results of the tests. A detailed finite element analysis and test results show that more stirrups are required for high strength concrete to obtain the same ductility as the normal strength concrete columns.

Key words: High strength concrete, stub columns, finite element analysis, fracture mechanics

1. INTRODUCTION

The high compressive strength of high strength concrete is especially advantageous in compressed members such as columns which can then be made more slender in design and, consequently, make economic benefits possible. An increase in compressive strength allows smaller cross-sections which require less concrete and permit more rentable floor space. The performance of structural elements made with high strength concrete has recently become a major concern for design engineers. There are many aspects, such as ductility, amount of reinforcement, effect of slenderness, and eccentricity of the applied load, that have to be

investigated to understand the behavior of the columns completely. Some researchers, *e.g.*, /1/-/5/, have studied short columns of normal and high strength concrete subjected to axial loading. However, the behavior of reinforced high strength concrete stub columns is not yet fully understood. Often the outcome of these studies results in empirical recommendations based on the individually performed test series. In view of the economic limitations that prevent complete test series to be carried out, it would be of great benefit to establish a suitable numerical model that reflects the structural behavior correctly.

An ongoing research program on reinforced columns made of high strength concrete combines experiments and numerical simulations. In the present study, 26 columns have been tested to failure under compressive loading. The parameters varied in this investigation were the concrete strengths, longitudinal reinforcement, stirrup spacing and eccentricity of the applied compressive load. In addition, the mechanical properties, such as the compressive and the tensile strength, the modulus of elasticity and the fracture energy, were measured in the experimental investigation. These material properties were incorporated into a model, where the material model for concrete was based on non-linear fracture mechanics. This model was, in turn, implemented in a non-linear finite element program in order to predict the responses of the concrete stub columns.

This paper describes the test program and the numerical aspect of the research program. The finite element model used in the analysis is presented, followed by verification against the experimental results. Observations of the failure mechanisms during the tests were made and some reasons why the columns failed under compressive loading are presented. Some effects of the confinement phenomenon are investigated and reported.

2. BEHAVIOR OF HIGH STRENGTH CONCRETE STUB COLUMNS

2.1 The Test Program

2.1.1 General

The test program consisted of two series. Twenty-two concrete stub columns, with a range of seven different compressive cylinder strengths varying from 33 to 99 MPa, were tested in the first series. The parameters varied in this series were concrete strength, stirrup spacing and reinforcement strength. In the second test series, four high strength concrete columns, with a compressive cylinder strength of 105 or 110 MPa, were tested. This test series was carried out as a complementary investigation to study the effects of different load eccentricities. Table 1 shows the different parameters and Figure 1 the geometry and details of the different configu-rations. For detailed information about the test program, see /6/ and /7/.

Table 1 Details of columns. Configuration u denotes unreinforced concrete.

Column group	Length [mm]	Config.	Stirrup spacing [mm]	Eccentricity [mm]
A	500	a	100, 180	0
B	800	b, c	130, 240	0
C	800	b	130, 240	0
D	900	u, d, d, d	50	0, 0, 90, ∞

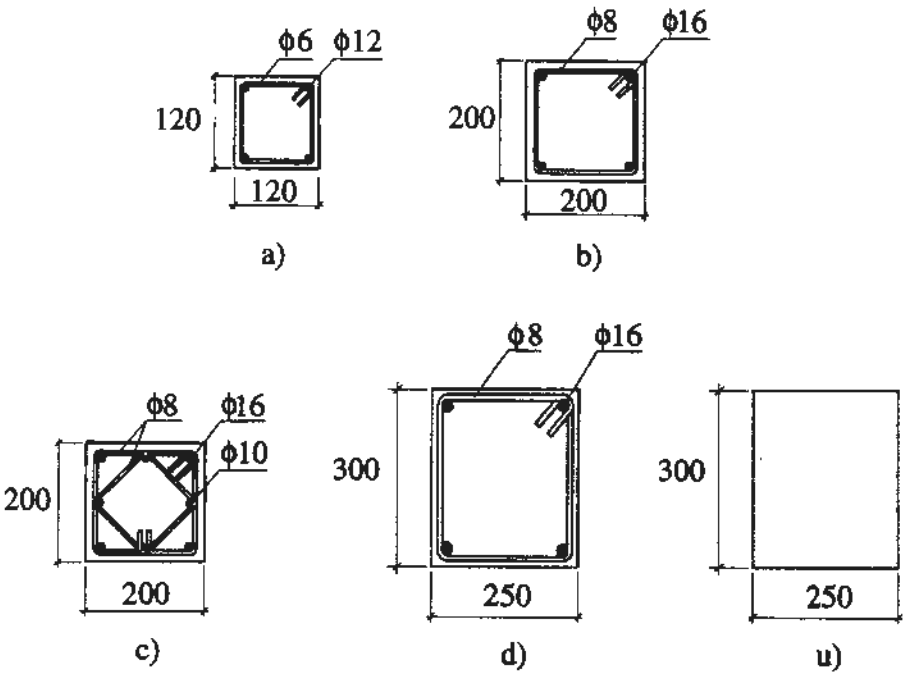

Figure 1 Concrete columns: geometry and details of configurations a), b), c), d) and u).

2.1.2 Material properties

The concrete mixes, designed with target compressive cube (150 mm) strengths of 50 and 120 MPa, were produced at the structural engineering laboratory at Chalmers University of Technology. Silica fume and plasticizer were used in the high strength concrete mixes to obtain high strength, workability, and reduction of fine particle segregation. The detailed concrete composition and hardened concrete properties are described in detail elsewhere, see /6/. The column specimens were cast horizontally in steel forms. The concrete was thoroughly vibrated by means of an internal vibrator.

Deformed bars of the Swedish qualities Ks40S and K500 were used as the lateral reinforcement, while Ks60 and K500 were used as the longitudinal reinforcement, see Table 2. The mechanical properties of the reinforcement are presented in Figure 2. All of the stirrups were anchored with 135° bends extending approximately 70 mm into the confined concrete core.

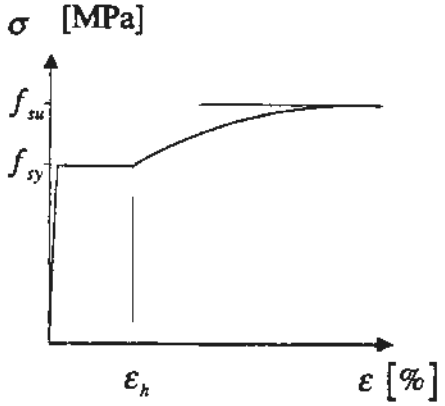

Reinforcement bar	A_s [mm²]	f_{sy} [MPa]	f_{su} [MPa]	ε_h [%]	E_s [GPa]
Ø16 Ks60	199	636	721	2.2	207
Ø16 K500	181	628	720	2.7	212
Ø12 Ks60	112	684	820	2.1	207
Ø10 Ks60	78	658	744	2.4	213
Ø8 K500	51	545	645	2.5	212
Ø8 Ks40S	50	466	607	4.0	221
Ø6 Ks40S	29	512	631	-	216

Figure 2 Mechanical properties of the reinforcement bars.

2.1.3 Test set-up

The stub columns were loaded between two rigid loading plates, see Figure 3, in all cases but one. At the four corners of the specimen, the vertical displacement of the lower movable loading plate of the column testing machine was measured in relation to the upper plate. The recorded data from the strain gauges, the vertical displacement from the displacement transducer and the corresponding axial load data from the hydraulic press were fed into a data acquisition system. In addition, the load-vertical displacement curve was continuously recorded on an xy-plotter during the test. Furthermore, for the eccentrically loaded stub column, see Figure 3b, the horizontal displacement was measured at three points. In group D, one high strength concrete column was tested subjected to pure bending using hydraulic jacks to apply the loads, see Figure 4. Displacements in the bending direction were measured by five displacement transducers.

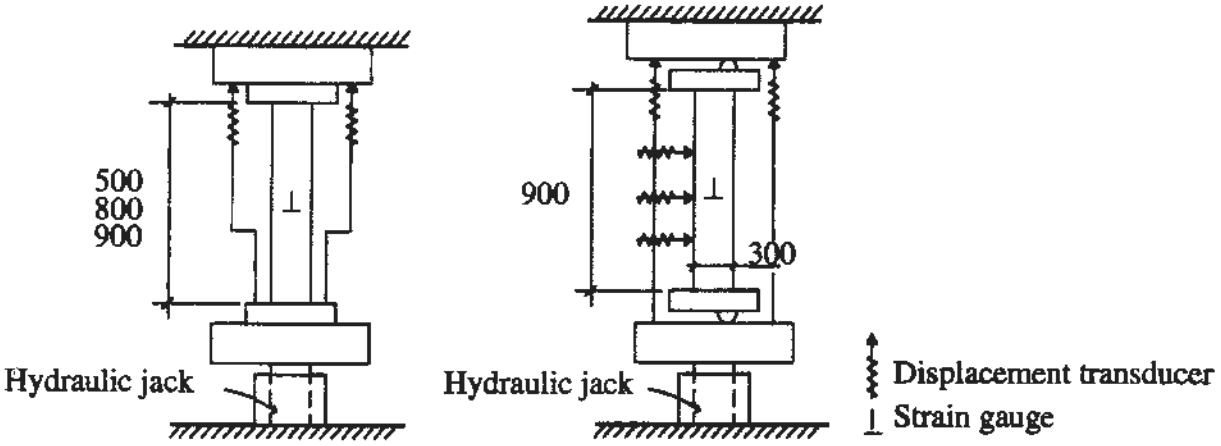

Figure 3 Instrumentation and measuring equipment on a) the centrically loaded stub columns and b) the stub column of group D loaded with an initial eccentricity of 90 mm.

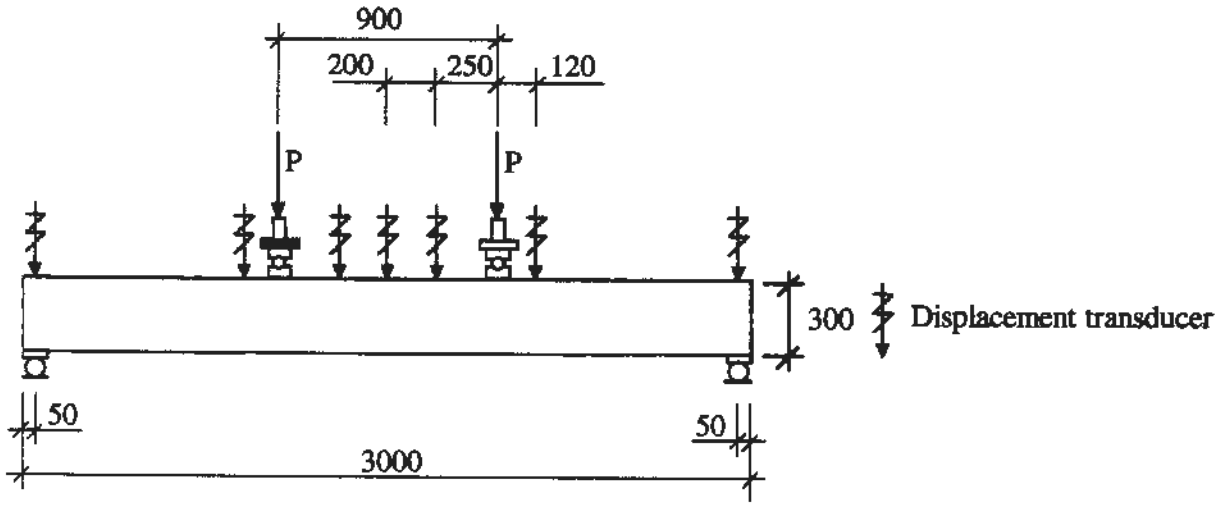

Figure 4 Instrumentation and measuring equipment on the high strength concrete column (#26) subjected to pure bending.

2.1.4 Test results

The columns were tested when they had reached an age of approximately 28 days. The duration of each test was approximately forty-five minutes.

In Table 2 the results from the stub column tests are presented. The length of the specimens in group A is 500 mm; in groups B and C, 800 mm, and group D, 900 mm, see Table 1. The concrete was either of normal (N) or of high (H) strength concrete. The compressive cylinder strength, $f_{c,cyl}$, and the compressive cube strength, $f_{c,cube}$, refer to compression tests on specimens of sizes ϕ150 x 300 mm (SS 13 72 30) and 150 x 150 x 150 mm (SS 13 72 10), respectively. Unless otherwise specified, Ks40S was used as lateral and Ks60 as longitudinal reinforcement.

Table 2 Results from the short stub columns.

Specimen no.	Column group	Concrete [N/H]	Long. reinf. ratio [%]	$f_{c,cyl}$ [MPa]	$f_{c,cube}$ [MPa]	Stirrup spacing [mm]	Stirrup config. [1]	Ecc. [mm]	Max. load, P [kN]
1	A	N	3	43	58	100	a	0	770
2	A	N	3	43	58	180	a	0	850
3	A	H	3	86	106	100	a	0	1390
4	A	H	3	86	106	180	a	0	1220
5	B	N	2	33	43	130	b	0	1650
6	B	N	2	33	43	240	b	0	1570
7 [2]	B	N	2	33	43	130	b	0	1620
8 [2]	B	N	2	33	43	240	b	0	1560
9	B	N	3	33	43	130	c	0	1900
10	B	N	3	33	43	240	c	0	1820
11 [3]	B	N	2	33	43	130	b	0	1570
12 [3]	B	N	2	33	43	240	b	0	1500
13	B	H	2	91	116	130	b	0	3920
14	B	H	2	92	112	240	b	0	4000
15 [2]	B	H	2	91	116	130	b	0	4010
16 [2]	B	H	2	92	112	240	b	0	3720
17	B	H	3	91	116	130	c	0	4250
18	B	H	3	92	112	240	c	0	4130
19	C	N	2	37	49	130	b	0	1810
20	C	N	2	37	49	240	b	0	1760
21	C	H	2	93	118	130	b	0	4030
22	C	H	2	93	119	240	b	0	4040
23	D	H	-	105	125	-	u	0	7670
24 [3]	D	H	1	105	125	50	d	0	6930
25 [3]	D	H	1	105	125	50	d	90	3060
26 [3]	D	H	1	110	132	50	d	∞	60

[1] See Figure 1.
[2] K500 was used as the longitudinal reinforcement.
[3] K500 was used as the lateral and the longitudinal reinforcement.

Typical load versus vertical displacement relations for a high strength concrete and a normal strength concrete short stub column are shown in Figure 5. Figure 6 shows a similar relation for the high strength concrete column #24. Due to the closer stirrup spacing, this column exhibited a less brittle behavior after the peak was reached, and the remaining load bearing capacity was larger compared with the load bearing capacities of the high strength concrete columns with stirrups further apart.

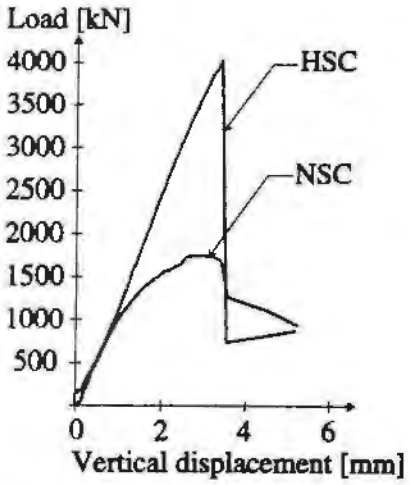

Figure 5 Load versus vertical displacement relation for a high strength concrete and a normal strength concrete stub column with stirrup spacing 130 mm. The columns are identical apart from the different concrete strength (#19 and #21).

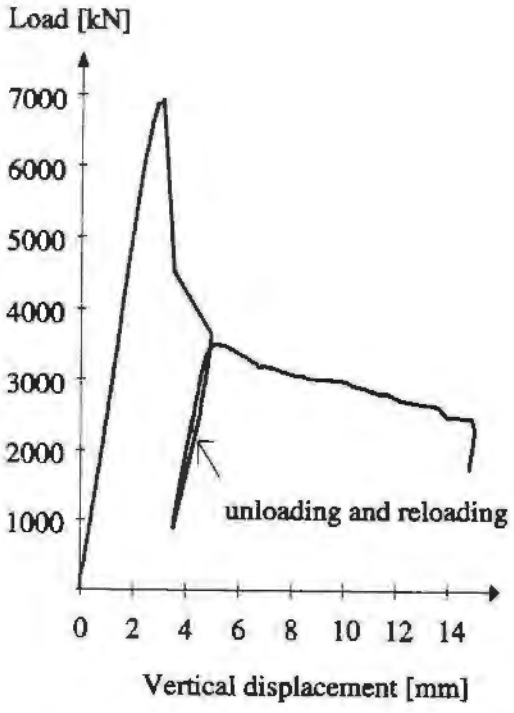

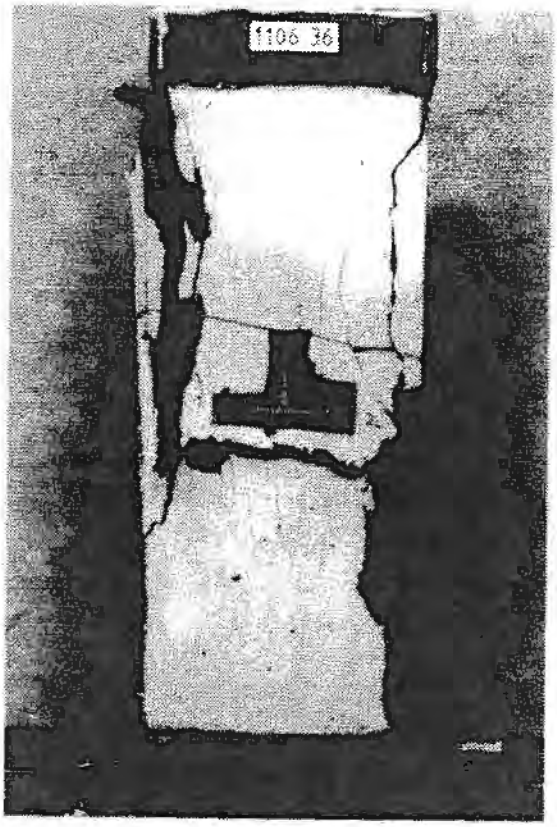

Figure 6 Measured load versus vertical displacement for a high strength concrete stub column (#24) with stirrup spacing 50 mm and a photo of the same column after completion of the test.

2.2 The Compression Failure of Unreinforced Concrete

Why do concrete columns fail in compression? In this subsection the failure of unreinforced concrete subjected to compressive loading will be discussed. Knowledge of this type of failure will contribute to the understanding of the failure process of reinforced concrete columns. To understand the compression failure at macro-level, one has to take advantage of the knowledge gained from the meso and micro-level. In Figure 7a, the load transfer and fracture mechanisms in particle composites subjected to compression are drawn schematically. The model, from van Vliet and van Mier /8/, is intended to represent cohesive particle composites, such as concrete and sandstone, in which the particles are bonded by a brittle matrix. The basic idea is that, due to particle interaction, tensile stresses appear in the matrix, which lead to fracture of the material. In the model described here, it is assumed that the aggregates have a higher Young's modulus than the surrounding matrix, and that the interface between the matrix and aggregates is the weakest link in the system. For high strength concrete, the aggregates and the surrounding matrix have about the same Young's modulus, which means that the cracks would be expected to run through the aggregate as well as the matrix. This is usually the case in static short-term tests. However, Taerwe /9/ has studied compression tests on high strength concrete cylinders where the loading system was controlled by the circumferential strain. The cylinders were sawn afterwards; the saw cuts indicated that fracture lines mainly pass along coarse aggregates as in normal strength concrete (except for flat shaped and weaker particles) and rarely run through the aggregates, as has been observed in the case of explosive failures. Hence, Taerwe suggested that the evenness of the fracture surface is related primarily to the speed of crack propagation; this was also observed in uniaxial tension tests carried out by van Mier /10/.

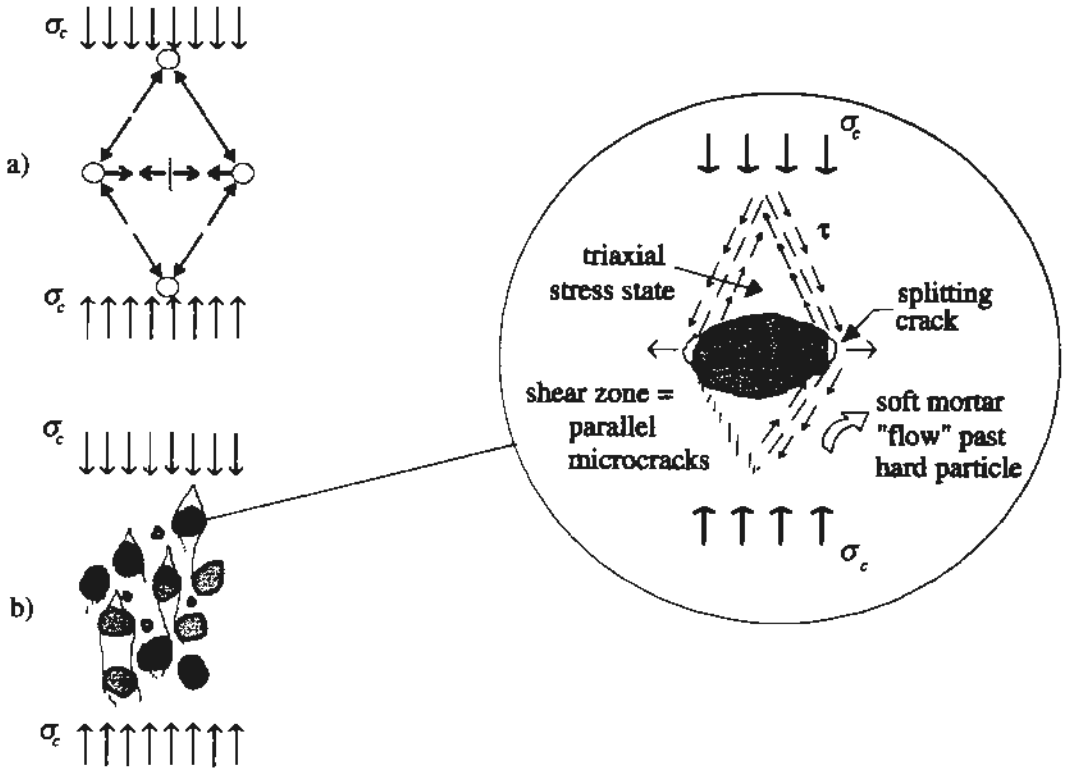

Figure 7 Failure in compression, in a) shown schematically for a configuration of four circular inclusions and b) a model for triaxially stressed areas above and below aggregates, based on /8/ and /11/.

The side faces of the aggregate particles show a combination of low compressive radial stresses (decreasing into tensile at the midpoint) and rather high shear stresses, see Figure 7b. Markeset /11/ suggests that this combination may initiate microcracking at the interface between the aggregate and cement paste (bond cracks). On the parts of an aggregate particle surface that are under radial compressive stress, the crack faces of the bond crack can neither open nor close: they can only slide.

When sliding between the aggregate and matrix starts, the dilating regions induce tensile stresses which, again, lead to increased bond cracking. At a certain load level, the bond crack will propagate into the matrix (cement paste). Considerably less bond cracking occurs in high strength concrete than in normal strength concrete. This is a result of the low water-cement ratio, which greatly increases the tensile capacity as well as the modulus of elasticity of the cement paste and also increases the bond strength between the cement paste and aggregate phases. At approximately 40% of ultimate stress for the normal strength concrete and 60 to 70 % for high strength concrete, the bond cracks start to extend into the cement paste under the action of longitudinal shear and lateral tension, see Figure 7b. Although the formation of these cracks does not alter the stability of the system, it could allow the aggregate particles to slide relative to the cement paste, thus contributing to the non-linearity of the axial stress-strain curve.

For normal strength concrete, the cement paste cracking becomes significant above about 75% of the ultimate strength. High strength concrete first shows significant cement paste cracking at a higher stress level, due to increased bond strength. The cement paste cracks become unstable when more stored energy is released by their formation than the amount that is required for propagation of a stable crack. At this stress level, the lateral strain increases at a higher rate than the axial strain, due to the extensive cement paste cracking. For ordinary concrete, dilatation and associated volume increase are registered. However, the more homogeneous the concrete type is (with regard to the elastic properties of the aggregate and the binder), the smaller this increase in volume will be.

Structural compressive failure is more complex than tensile failure as it is always accompanied by lateral deformations which are responsible in general for the boundary effects. At the meso level, the fracture process can be described by the opening and sliding of microcracks which, by increased loading, grow into macrocracks, some axial and some inclined. This means that the final failure mechanism should include both axial splitting and inclined (shear) band formations, see Figure 8. Figure 8 also includes a photo of a tested unreinforced high strength concrete column after failure. One main vertical splitting crack is clearly visable as well as an inclined band. The failure was sudden and brittle. The latter observation could, however, be explained by the load controlled manner in which the load was applied. It is important to realize that the influence of each failure mode probably also depends on concrete material factors such as concrete composition, type of aggregate and maximum size of aggregate.

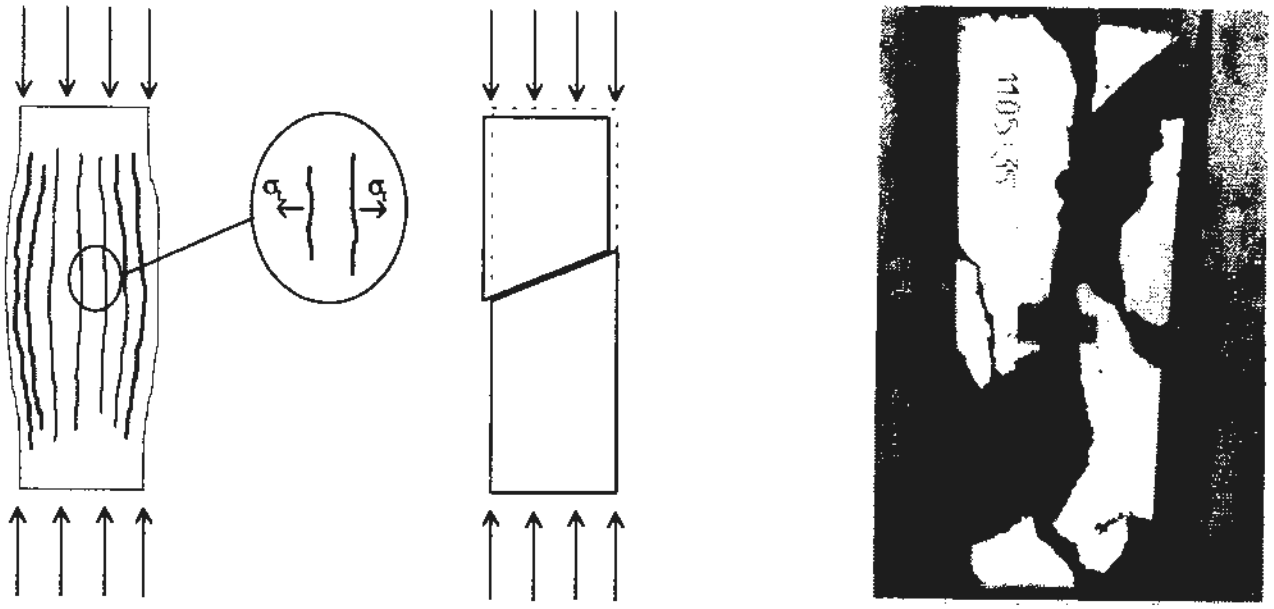

Figure 8 Longitudinal tensile cracks, sliding failure in a localized shear band, /11/, and a photo of an unreinforced concrete column (#23) after failure.

Van Vliet and van Mier /8/ observed that when considering a complete specimen, the strength in compression depends very much on the type of loading plate used in the experiment as well as on the size of the specimen. These variations in strength are caused by the presence of a triaxially stressed zone in the specimen. In fact, the significance of the boundary conditions and the size of a specimen suggests the conclusion that it is a structural property rather than a material property which is determined in a compressive cube or cylinder experiment.

2.3 Failure of Reinforced Concrete

Reinforced and unreinforced concrete differ in type of failure. Unreinforced concrete exhibits a more sudden, and in many cases, explosive type of failure. The reinforced concrete specimens display a more gradual type of failure because of the positive effects of the reinforcement. In a structural member, the passive confinement is provided by the lateral steel. This steel induces compressive confining stresses on the concrete core, because of its elongation, caused by the expansion of the concrete (Poisson's effect), see Figure 9. When the axial strain increases, the confining pressure in the two transverse directions increases, and the strength of the concrete core in the principal loading direction is enhanced as well. When the confining steel yields, irrespective of the lateral expansion of the concrete, the confining pressure remains fairly constant and only increased strain in the strain hardening region of steel will result in a limited further increase of confining pressure.

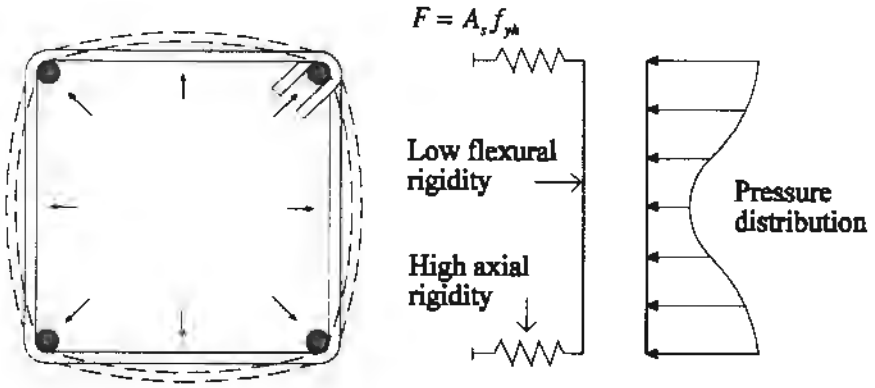

Figure 9 The lateral expansion of concrete under axial compression and the response of a stirrup with high restraining action at the corners, /2/.

When a reinforced concrete column is subjected to axial load, the concrete cover is unconfined and becomes ineffective after its compressive strength has been reached. The concrete core continues to carry stresses under high strain. The increase in strain of confined concrete can be calculated on the basis of the "effectively confined" concrete area. This area is less than the normal core area bounded by the center line of the perimeter tie and it is determined by tie configuration and spacing. The difference between the effectively confined and unconfined concrete may be represented in the form of a series of arches spanning between the reinforcement bars, see Figure 10.

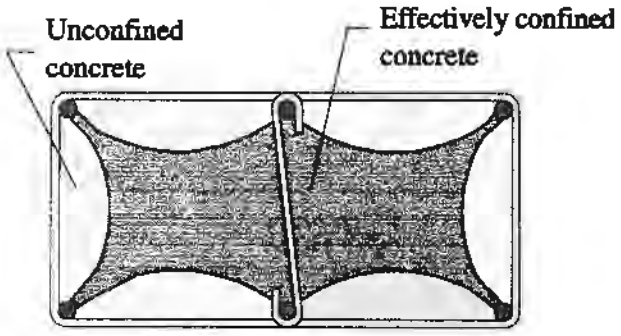

Figure 10 The concrete section divided into unconfined concrete and effectively confined concrete. Compressive arches between the longitudinal bars are shown.

In the failure of reinforced members, the reinforcement cage can form a natural vertical plane of separation. This appears to be the weakest part of many specimens, especially for high strength concrete columns, but also for normal strength concrete specimens with denser lateral reinforcement configuration. The failures of the normal strength concrete columns in the tests were gradual, *i.e.*, the cover spalled off slowly over quite a long period of time, and a significant post-peak curve was obtained. The columns of high strength concrete exhibited a sudden explosive type of failure. It appears that the high compressive stresses in the concrete cover led to buckling of the cover. The stirrups that were present between the core and the cover formed a natural plane of separation. This led to a complete loss of concrete cover capacity. Strength reduction occured when the confinement of the core was not sufficient to compensate for the instability of the cover. This was the case for all of the high strength concrete columns in the first test series. The specimens failed immediately after the first maximum axial load was reached, indicating that the number of lateral ties was not enough to provide sufficient lateral

confinement, even with the denser stirrup configuration. At the end of the tests, after the maximum load had been reached, some of the longitudinal bars buckled. However, when a closer stirrup spacing was used in the complementary study, part of a post-peak curve was obtained. It is interesting to observe that the unreinforced high strength concrete column, #23, obtained a higher bearing capacity than the reinforced one, #24. This can probably be explained by the weakness plane created by the reinforcement cage. The differences between the failure of the normal and the high strength concrete columns can be seen in Figure 11.

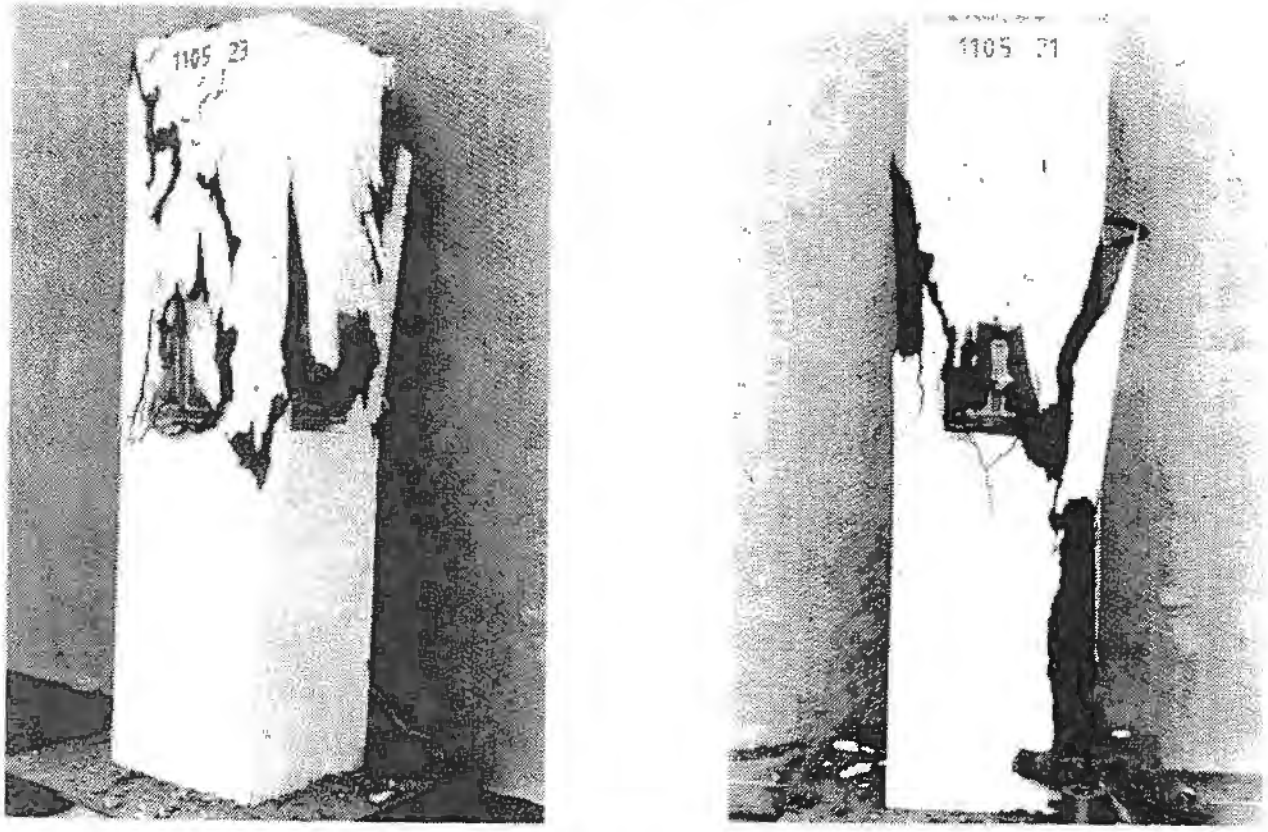

a) b)

Figure 11 The photos show the failure of a) normal strength concrete (#5) and b) high strength concrete (#17) stub columns.

Tests have shown (*e.g.*, /1/) that the confinement of concrete by suitable arrangements of transverse reinforcement results in a significant increase in both the strength and the ductility of compressed concrete. In particular, the strength enhancement from confinement, and the resulting slope of the descending branch of the concrete stress-strain curve, show a considerable influence on the flexural strength and ductility of reinforced concrete columns. Accordingly, it is important to have accurate information about the complete stress-strain curve of confined concrete in the design process.

2.4 Effects of Stirrup Spacing

An important aspect in the failure of reinforced concrete columns is the effects of stirrup spacing on the inelastic buckling of longitudinal reinforcing bars. A numerical simulation carried out by Mau /12/ showed that the load-carrying capacity is greatly enhanced beyond the yielding point if

the tie spacing is smaller than a value defined by a critical spacing-longitudinal bar diameter ratio (S/D ratio), for reinforcing steels that exhibit an elasto-plastic-hardening behavior under monotonic loading. For reinforcement bars of grade 60 (corresponding to a yield strength of approximately 410 MPa), it was found that the critical value lies within the range of 5 to 7. In column design, when the maximum allowed S/D value of 16 is used (according to BBK 94 and ACI 318-89 for vertical spacing of lateral ties) the longitudinal bars are expected to achieve the yield load. At yielding, the steel buckles and the post-buckling path is clearly unstable, with decreasing load-carrying capacity thereafter.

Mainly three different stirrup spacings, with the S/D ratio equal to 15, 8 and 3, were used in the tests of the present study. Some observations could be regarding the stirrup spacings. The reinforcement bars had reached yielding at maximum load for all the centrically loaded columns. However, there was a clear difference in the behavior of the normal and the high strength concrete columns. Due to the separation plane between the reinforcement cage and the concrete cover, no post-peak curves were obtained for the high strength concrete columns with the S/D ratio equal to 15 and 8. But when the S/D ratio was reduced to 3 a post peak curve was obtained. For the normal strength concrete columns, post-peak curves were captured for all ratios. This leads to the conclusion that a closer stirrup spacing is needed when high strength concrete is used to take advantage of the higher load bearing capacity.

The failure of concrete in compression is quite a complex problem. Many parameters and loading situations will have to be investigated to understand fully the structural behavior of reinforced concrete columns in compression. In order to propose recommendations for practical applications in design, it is necessary to understand why and how concrete columns fail. A finite element model based on non-linear fracture mechanics combined with experimentation is believed to be a powerful combination in analyzing the behavior of reinforced concrete columns. This kind of analysis has been carried out and is presented in the next sections.

3. FINITE ELEMENT ANALYSIS

3.1 General

Due to economic limitations that prevent complete test series being carried out, it would be of great benefit to establish a suitable numerical model that reflects the structural behavior of concrete columns correctly. One of the aims of this study was to establish finite element models, with material models for concrete based on non-linear fracture mechanics, that can simulate the failure mechanism of the columns. Together with the experiments, the non-linear finite element analyses will facilitate a better understanding of the mechanical behavior of the failures, including the post-peak behavior.

3.2 The Material Models

3.2.1 Fracture mechanics

Conventional fracture mechanics deals with the risk of failure of a material due to the propagation of a single crack and is widely used, for example in the case of fatigue in metals. It is based mainly on linear elastic theory, but includes different techniques to take energy

absorption, plasticity and other phenomena near the crack tip into account. However, the methods developed in conventional fracture mechanics are not, as a rule, suitable for concrete structures. The analysis of the behavior of concrete structures must include the influence of fracture toughness. To carry out this type of analysis, which is a better way of handling materials such as concrete, non-linear fracture mechanics was developed. Today, non-linear fracture mechanics is used in several finite element programs to form constitutive models for simulating the behavior of reinforced concrete. With such models the mechanical behavior of the structure, including the effect of progressive cracking, can be simulated more accurately than with conventionally used methods.

The models in this study were designed using the non-linear finite element program ABAQUS, /13/. To model reinforced concrete, the program combines standard elements of plain concrete with a special option, called rebar. This option strengthens the concrete in the direction chosen in order to simulate the behavior of a reinforcement bar. The rebar option is used with metal plasticity models to describe material behavior of the reinforcing steel. With this approach, the material behavior of the plain concrete is considered independently of the reinforcement. The interaction between the reinforcement bars and the surrounding concrete cannot be modeled in a suitable way with the current version of the program.

3.2.2 Constitutive models for concrete and reinforcement

Cracking is a very important phenomenon in the analysis of concrete structures. Here, the smeared crack approach has been chosen to model cracked reinforced concrete. The localized non-linearity of the material is smeared out and the response in tension can be described in terms of stress-strain relations for the material including the cracks. Cracking is assumed to occur when the stresses reach a failure surface called the "crack detection surface", see Figure 12. The failure surface is a Coulomb line written in terms of the first and second stress invariants. Once a crack has been detected, its orientation is stored and a second crack at the same point may only form orthogonal to this direction. Prior to cracking, the concrete is modeled sufficiently accurately in tension as an isotropic, linear elastic material.

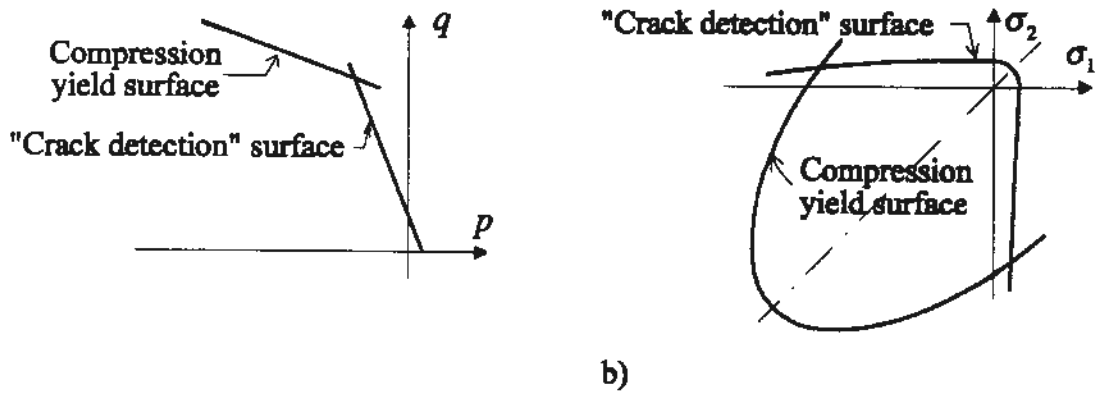

Figure 12 Compression yield surface and crack detection surface a) in the p-q plane (p = hydrostatic stress, q = deviatoric stress); and b) in plane stress, see /13/.

When the principal stress components are dominantly compressive, the response of the concrete is modeled by an elastic-plastic model. The elastic stage is limited by a Drucker-Prager yield

surface. Once yielding has occurred, an associated flow rule together with isotropic hardening are used. The uniaxial stress-strain relations in compression, used in the analyses, were determined by tests on cylinders (ϕ150 x 300 mm), cast with concrete from the same batch as the columns. Poisson's ratio was approximated to be 0.2. The fracture energy was determined from RILEM beams, and was together with the tensile strength used to calculate the tensile softening relation.

The reinforcement bars were modeled by a linear elastic, perfectly plastic material model. The modulus of elasticity and the yield strength were determined by tension tests for each steel quality and Poisson's ratio was set to 0.3.

3.3 Numerical Studies

To be able to study the effect of confinement it is necessary to analyze the columns using three-dimensional solid elements. While a solid element model requires more computational effort than, for example, a beam element model, it is possible to simulate the effect of transversal reinforcement. In this model, three-dimensional 8-node solid elements were used. Figure 13 shows the finite element (FE) mesh and the boundary conditions for the solid element models.

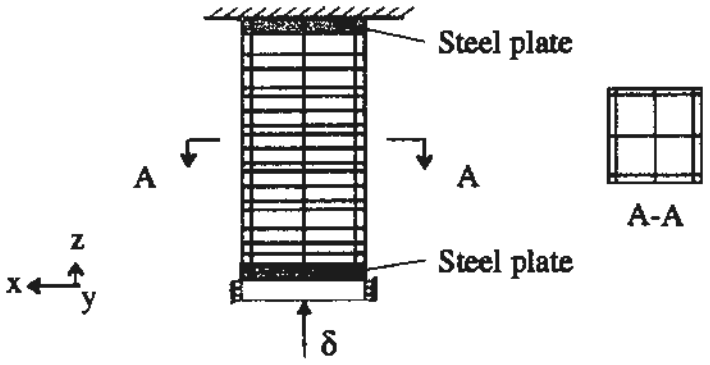

Figure 13 Finite element mesh and boundary conditions used in the solid element model of the short stub columns.

The Newton-Raphson iteration method is the standard method in ABAQUS and is usually sufficient for monotonic loading. Analyses of reinforced concrete structures, however, often exhibit local maximum points in the load-displacement curve with snap-through or snap-back behavior, see /14/. To overcome this situation, the load was applied as a deformation using the Newton-Raphson model together with a line search approach. Numerical convergence problems were, nevertheless, found in several cases for the iterative solution technique, especially when trying to obtain the descending branch of the load-displacement relation.

4. COMPARISON OF THE FE-ANALYSIS WITH THE TEST RESULTS

The benefit of carrying out both computer simulations and experiments is that the advantages of each method can be combined and, therefore, a more thorough understanding of the problem is gained. However, to be able to rely on the results of the computer simulations, these must be verified against experiments. The test results involving two stub columns, one in high strength

concrete [1](#13) and one in normal strength concrete [1](#5), were compared to the corresponding results of the finite element analysis. The load-displacement relations were compared to determine the structural response of the stub columns. These comparisons are shown in Figure 14. As can be seen in these figures, the finite element models simulate the structural behavior well. Even if the predicted value of the maximum load is somewhat too high, the general behavior has been captured. Therefore, it is plausible to analyze the results of the analysis in further detail.

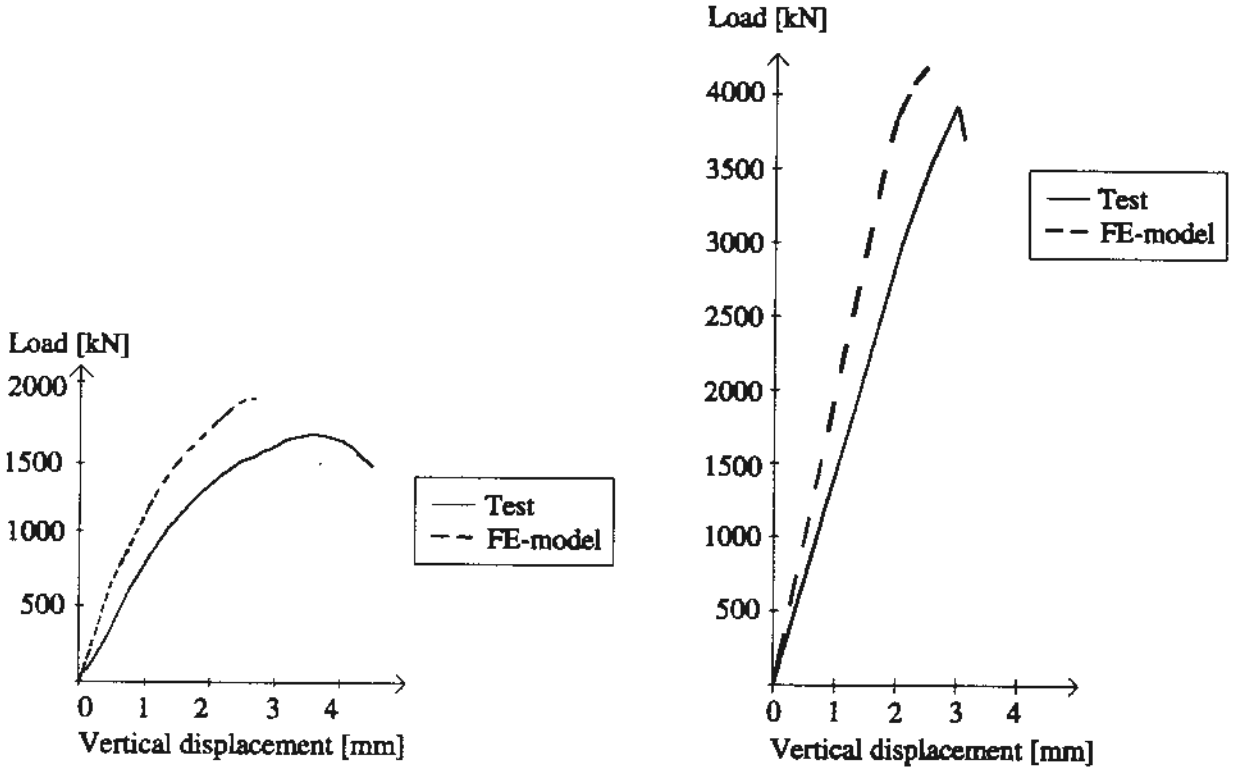

Figure 14 Comparison of an FE-analysis with solid elements and the test of a a) normal strength concrete stub column (#5) and b) a high strength concrete stub column (#13).

One of the aims of this study was to determine whether any positive effect was caused by the stirrups. Figure 15 shows the stress-strain relation of a normal strength concrete stub column at mid-height. The curves are from three different elements, one at the corner of the concrete cover, one on the side of the concrete cover, and one from the inner confined core. These curves indicate possible effects of confinement, *i.e.*, the maximum stress of the core is enhanced due to the lateral reinforcement.

[1] Referring to Table 2

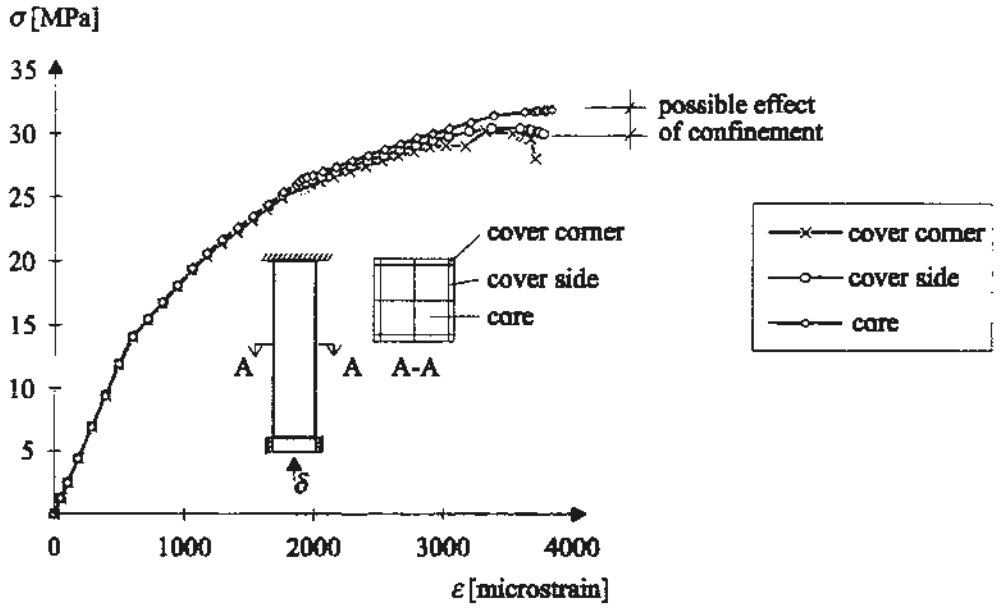

Figure 15 Possible effects of confinement shown by the stress-strain relations from an FE-analysis for elements at mid-height of a normal strength concrete stub column.

A similar analysis was carried out for the stub columns in high strength concrete, see Figure 16. The effect of confinement was detected. However, it was not as pronounced as in the case of the normal strength concrete stub column.

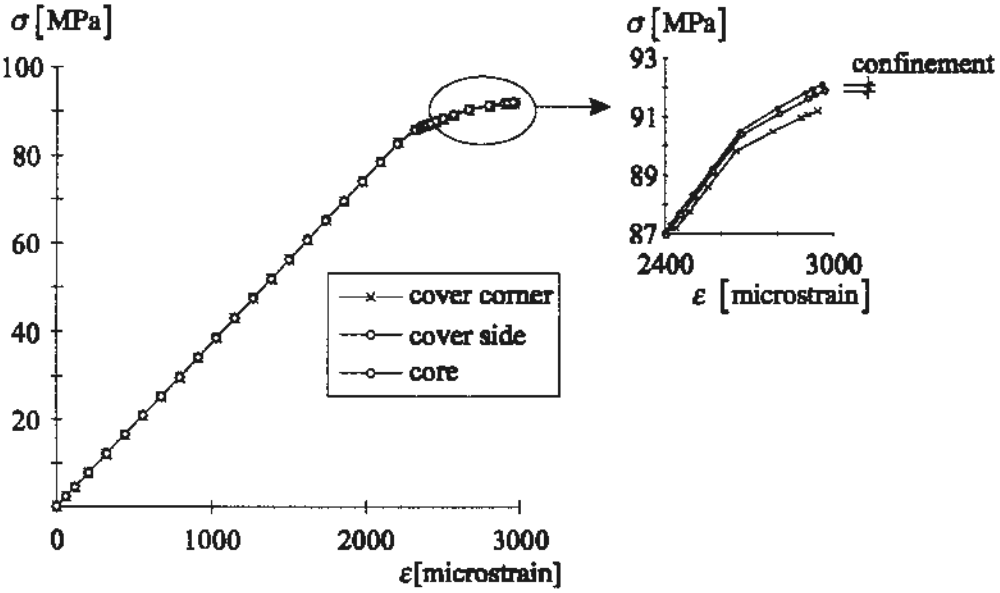

Figure 16 Possible effects of confinement shown by the stress-strain relations from an FE-analysis for elements at mid-height of a high strength concrete stub column.

To study the compressive arches, due to the confinement effect, as shown in section 2.3, a more detailed analysis of the same columns has been carried out. The element mesh of this analysis is shown in Figure 17. One forth of the cross section was modeled. Figures 18 and 19 show the vertical stress distribution between the stirrups. In both cases, the distribution is at maximum load.

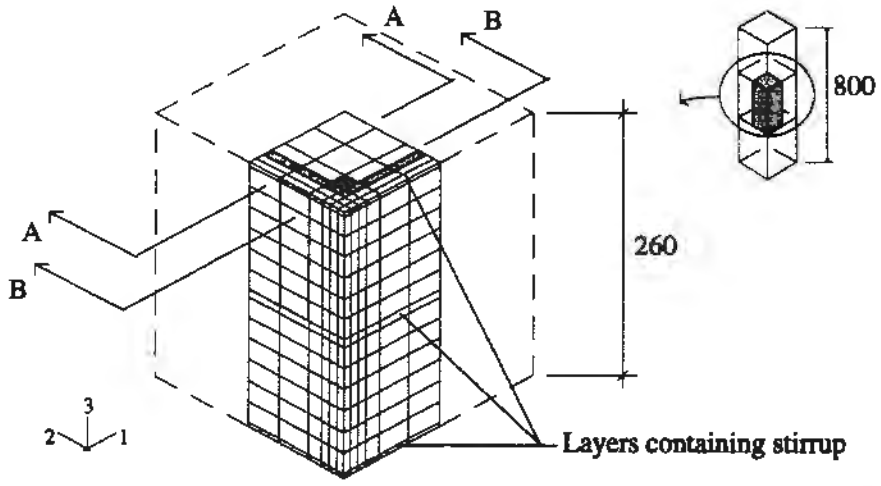

Figure 17 Element mesh of one fourth of the cross section. The height of the model is 260 mm.

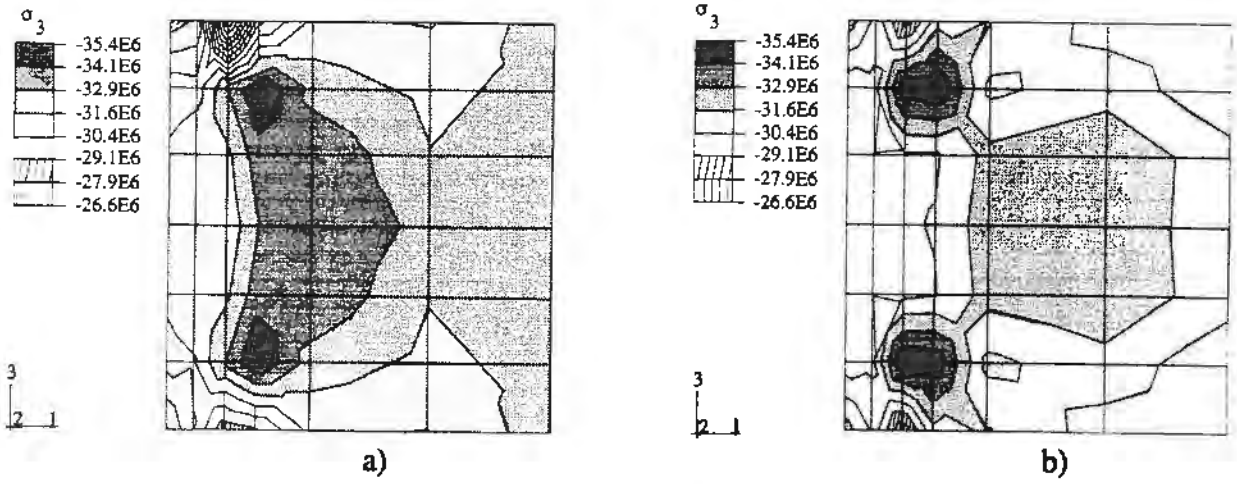

Figure 18 The effect of confinement for a normal strength concrete stub column at vertical sections a) A-A and b) B-B between two stirrups.

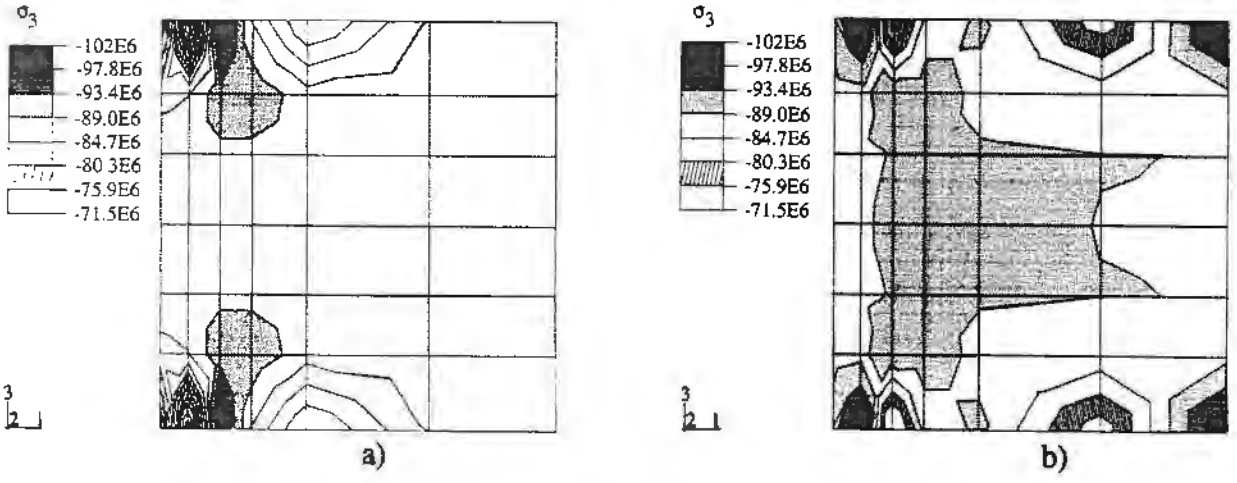

Figure 19 The effect of confinement for a high strength concrete stub column at vertical sections a) A-A and b) B-B between two stirrups.

5. DISCUSSION

From the results of the FE-analysis, it has been observed that the size of the specimen and the loading rate are important parameters. The compressive material parameters that were used, obtained from a standard cylinder, usually gave too high a load bearing capacity, see Figure 14, and /6/. Nevertheless, the results of the FE-analysis gave quite an accurate reflection of the structural behavior of the stub columns. To improve the accuracy, more realistic material models for concrete and a finer element mesh are needed.

The results of the FE-analysis show an enhancement in stress not only of the concrete core, but also in the concrete adjacent to the stirrups. Between two stirrups, the concave arch has its minimum, implying that the confinement effect is lowest at this point. This can be seen in Figures 18 and 19. In these figures, it can be observed that the confinement effect is more pronounced in the case of normal strength concrete. It appears as if more transversal reinforcement is required for the high strength concrete columns to achieve the same positive effect of confinement as that of the normal strength concrete columns. This supports the observations made in this test series and in other studies, *e.g.*, /4/.

Many recommendations regarding how to calculate the enhancement of stress due to the confining action assume that the stirrups yield at maximum load. However, in reality, this yielding depends very much on the spacing of the stirrups. It has been observed, both in the experiments and the analysis, that the stirrups did not reach yielding at maximum load for two of the three stirrup spacings tested, namely, S/D equaling 15 and 8. In the complementary study with S/D equal to 3, the stirrups were very close to or actually yielding when the high strength concrete column reached its maximum load. Evidently, it is important either to design the columns with a proper stirrup spacing to ensure that the stirrups yield at maximum load or to use the actual strain when calculating the increased strength.

6. CONCLUSIONS

The results of the tests of the twenty-six short stub columns show that the load bearing capacity increased with increased compressive strength. The failures of the short stub columns of normal strength concrete were gradual and a good part of the post-peak curves was obtained. The short stub columns in high strength concrete, had a sudden explosive type of failure, except those with a denser stirrup spacing that exhibited a less brittle failure. It appears that the high compressive stresses in the concrete cover led to buckling of the cover. The reinforcement that was present between the core and the cover formed a natural plane of separation. This led to a complete loss of concrete cover capacity. Strength reduction occured when the confinement of the core was not sufficient to compensate for the instability of the cover. There are reasons to believe that with a very dense reinforcement configuration, a higher bearing capacity can be reached after the loss of the concrete cover, due to the triaxial stress state created by the reinforcement cage.

A finite element (FE) model was established to study the effect of confinement of normal and high strength concrete columns. The enhancement in strength of the concrete core, due to the confining effect of the stirrups, was detected in the FE-analysis, both in the case of normal strength and high strength concrete. However, it was observed that the confining effect was less for the higher concrete strength.

A more detailed analysis was carried out to study the effect of the confining stirrups. Two main conclusions can be drawn from this analysis. Firstly, the confining effect of the stirrups was greatest in the area around the stirrups and lowest between two adjacent stirrups. Secondly, even if a confining effect was detected for the high strength concrete columns, this was not as large as for the normal strength concrete columns. Therefore, to receive the same positive effect, more stirrups are needed for high strength concrete columns. This observation is in agreement with findings of other researchers, *e.g.*, /1/.

In the tests and in the FE-analysis, the stirrups did not reach yielding. Usually, when calculating the enhancement in strength, the stirrups are assumed to yield at maximum load. This leads to an overestimation of the strength. To estimate the strength correctly, it is necessary to use the actual strain or to design the reinforcement configuration so that yielding is reached at maximum load.

One possible avenue for future research is to determine the strength of the core and the cover and give a recommendation for design. In this study, the vertical plane of separation between the reinforcement cage and the concrete cover, detected in the tests of the high strength concrete columns, has not been modeled. In future research, it might be of interest to simulate this plane to ascertain more accurately the characteristics of the failure process.

7. ACKNOWLEDGEMENT

This project is a part of a national research project treating the properties of high strength concrete. The authors wish to express their gratitude to the Swedish Building Council, Nutek and the building companies Strängbetong AB, NCC, Skanska, Cementa, Elkem Materials and Euroc Beton for financing this project.

8. REFERENCES

/1/ Cusson D. & Paultre P., "High-Strength Concrete Columns Confined by Rectangular Ties", Journal of Structural Engineering, Vol. 120, No. 3, March, 783-804, 1994

/2/ Saatcioglu M. & Razvi S.R., "Strength and ductility of confined concrete", Journal of Structural Engineering, ASCE, 118(6), 1590-1607, 1992

/3/ Mander J.B., Priestley J.N & Park R., "Observed stress-strain behavior of confined concrete", Journal of Structural Engineering, ASCE, 114(8), 1827-1849, 1988

/4/ Ahmed S.H. & Shah S.P., "Stress-strain curves of concrete confined by spiral reinforcement", ACI Journal, Proceedings V. 79, No. 6, Nov.-Dec., 484-490,1982

/5/ Bjerkeli L., Tomaszewics A. & Jensen J.J., "Deformation properties and ductility of high strength concrete", Utilization of High-Strength Concrete - Second International Symposium, SP-121, American Concrete Institute, Detroit, 215-238, 1990

/6/ Claeson C., "Behavior of reinforced high strength concrete columns", Licentiate thesis, Publication 95:1, Division of Concrete Structures, Chalmers University of Technology, Sweden,1995

/7/ Segesten E. & Waller E., "Behaviour of eccentrically loaded short stub columns of high strength concrete", Master's thesis, Diploma work 95:2, Division of Concrete Structures, Chalmers University of Technology, Sweden,1995

/8/ Van Vliet M. R. A., van Mier J.G.M.,"Comparison of lattice type models for concrete under biaxial loading regimes", Size-scale effects in the failure mechanisms of materials and structures, Carpenteri A. (Ed.), E&FN Spon, London/New York (in press)

/9/ Taerwe L., "Emperical analysis of the fracture process in high strength concrete loaded in uniaxial compression", Fracture and damage of concrete and rock - FDCR-2, Rassmanith H.P. (Ed.), E&FN Spon, pp. 122-134, 1993

/10/ Van Mier J.G.M., "Strain softening of concrete under multiaxial loading conditions". Dissertation, Eindhoven University of Technology, Eindhoven, The Netherlands, 1984

/11/ Markeset G., "Failure of concrete under compressive strain gradients". Dissertation, University of Trondheim, Trondheim, Norway, 1993

/12/ Mau S.T., "Effect of tie spacing on inelastic buckling of reinforcing bars", ACI Structural Journal, V. 87, No. 6, Nov.-Dec., pp 671-677, 1990

/13/ HKS, Hibbit, Karlsson & Sorensen INC. (1992). ABAQUS, Theory Manual, Version 5.2. HKS, Providence, Rhode Island 02906 USA

/14/ Crisfield M.A., "Non-Linear Finite Element Analysis of Solids and Structures", V. 1, John Wiley Sons Ltd., Chichester, 345 pp, 1991